Available online at www.sciencedirect.com
ScienceDirect
Energy Reports 8 (2022) 665–674
www.elsevier.com/locate/egyr

TMREES22-Fr, EURACA, 09 to 11 May 2022, Metz-Grand Est, France

A CFD Energetic study of the influence of the panel orientation in Open Joint Ventilated Façades

M.J. Suárez[a], M.N. Sánchez[b,*], E. Blanco[a], M.J. Jiménez[b,c], E. Giancola[b]

[a] Universidad de Oviedo, EDZE (Energía), Campus de Viesques, 33271 Gijón, Asturias, Spain
[b] Energy Efficiency in Buildings Unit, Department of Energy, CIEMAT, 28040 Madrid, Spain
[c] Plataforma Solar de Almería, CIEMAT, Carretera de Senés s/n, Tabernas, 04200 Almería, Spain

Received 20 June 2022; accepted 19 July 2022
Available online 1 August 2022

Abstract

The arrangement of the panels in Open Joint Ventilated Façades (OJVF) is a potential factor in improving the energy efficiency of this building system. The distribution of joints in the façade influences the behaviour of the air flow in the channel which in turn could affect the overall heat exchanges with the envelope and thus the internal conditions of the building. Tiling panels can be installed on ventilated façades with different arrangement patterns according to the layout of the joints: lined up, staggered, stepped, diagonal or random, although manufacturers recommend a façade layout with in-line gaps to avoid costly façade maintenance. Thus, landscape and portrait layout with continuous joints are the most frequent arrangement in ventilated façades. This research assesses the benefit of the installation of OJVF panels in both layouts in order to reduce the cooling loads. Two real OJVFs with different panel arrangements, landscape and portrait, are analysed. Also, they are compared with a conventional façade with a sealed air cavity. All solutions are modelled and simulated using the commercial computational fluid dynamics software ANSYS FLUENT to evaluate the fluid-dynamic and thermal behaviour of the façades in summer and winter conditions. The energy performance of these solutions is evaluated, analysing different parameters such as panel's temperature, mean air velocity inside the cavity, fluid pathlines through the open joints and thermal flux in the air cavity and to the room. The airflow inside the cavity is mainly driven by thermal buoyancy in all façades but differs from bi-dimensional convective loops in conventional façades to three-dimensional complex and asymmetrical airflows in OJVFs. The results obtained show that both OJVF configurations perform much better than the conventional sealed façade, reducing the heat transfer into the room by 30% in the summer period. In any case, the landscape OJVF façade reduces the transfer in the same period to a minimum value of 7.3 W/m2, which is 3% less than the flux transferred through the vertical one. This small difference in the energy performance of OJVFs makes the choice of panel orientation more based on other criteria such as aesthetics.

Peer-review under responsibility of the scientific committee of the TMREES22-Fr, EURACA, 2022.

Keywords: Ventilated façades; Natural convection; CFD; PIV; Energetic analysis; Building energy

* Corresponding author.
E-mail address: nuria.sanchez@ciemat.es (M.N. Sánchez).

https://doi.org/10.1016/j.egyr.2022.07.114

Peer-review under responsibility of the scientific committee of the TMREES22-Fr, EURACA, 2022.

1. Introduction

Sustainable and versatile building envelopes [1,2] can contribute to reduce energy use during the lifecycle of buildings i.e. adaptive façades [3,4], ventilated roofs [5,6], the use of efficient shading devices [7] and the integration of external coatings in building retrofitting [8]. These constructive components must be then designed performance-oriented to optimize the interaction between indoor and outdoor environment [9,10] at the early design stages [11], i.e. Albatayneh [12] used genetic algorithms for the optimization of the building envelope in a residential building in Mediterranean climate. This goal can be achieved with high-performance solutions for the building envelopes, such as ventilated façades [13], which have become one of the most effective measures to reduce the radiation overheating in summer periods [14,15]. One of the main characteristics of these façades is the presence of a ventilated channel created between the internal and external layers of the building envelope [16]. Pastori et al. [17] revised the requirements and specifications that ventilated façades should fulfil. There is a great diversity of names for these solutions: ventilated walls, double skin façades, rainscreen, ventilated façades, and so on. Among them, the double skin façades have been widely studied [18–20]. Several analyses can be found about numerical or dynamic simulations [18,21,22], materials of diverse façade layers [23–27], different renewable energy systems installed in the façade, such as photovoltaic panels [28–30] or building integrated photovoltaic/thermal double façade solutions [31].

In residential buildings, the opaque ventilated façades are being widely implemented [32,33]. The main characteristics of these façades are the air cavity ventilated by means of small gaps in the lower and upper part of the cavity. About these façades, few scientific studies have been found [34,35]. The system operation has been experimentally assessed in Mediterranean climate conditions [36,37] and cold zones of China [38], under different façade orientations and at two states of windiness in summer [39] and winter reference days [40].

In this work, a particular opaque ventilated façade called “Open Joint Ventilated Façade” (OJVF) is evaluated. In this case, the external coat of the façade is composed of multiple panels separated by open joints and anchored to the building by means of a metallic structure. Research papers on these specific façades are rather scarce. Our research team has studied them numerically and experimentally. A laboratory model of OJVF with horizontal and vertical joints [41] was built based on previous simplified models [42,43]. In order to perform the velocity measurements, the Stereo-PIV methodology [44] was selected among different experimental techniques available for the airflow characterization [45]. The set-up of the laboratory was based on the studies applying the 2D-PIV technique to a horizontal OJVF model [46]. About the numerical studies, the commercial Computational Fluid Dynamic (CFD) code named FLUENT was used to develop and validate previous 2D and 3D models [47–49]. In both cases, proper boundary conditions have to be defined to lead to the best possible solution of equations system characterizing the behaviour of the façade. Also, different turbulence and radiation models were tested and validated.

However, an issue that still has not addressed in the installation of an open joint ventilated façade is the orientation of the panels. In this type of façades, as the air inlet and outlet take place through the joints throughout the height of the façade, not only at the lower and upper part of the air cavity as in the other ventilated façades, it is very important to know the most adequate orientation of the panels (landscape or portrait). In this paper, the thermal behaviour of OJVF with panels oriented landscape and portrait is analysed. The main objective of this paper is to accomplish the optimal orientation based on the maximization of both performance and energy efficiency.

2. Methodology

The impact of the panel layout (landscape or portrait) on the performance of the OJVF is numerically assessed in this paper. A numerical model has been developed using the CFD code ANSYS Fluent, and validated with the Stereo-PIV methodology in Sánchez et al. [47]. This model is employed to simulate two real OJVFs with the same layers and material properties, but with different panel arrangement: landscape and portrait. The thermal and fluid-dynamic behaviour of both orientations are analysed, considering both summer and winter conditions.

2.1. Geometry and meshing

Regarding geometry, the height of both façades is 2.4 m, a usual value of the distance between two adjoining floors. The ventilated air cavity is 5-cm-wide and the outer skin is composed of 40 × 80 cm ceramic panels with a thickness of 2 cm. There are 5 mm horizontal and vertical open joints between the panels, with the same total length of joints in both façades. In the model, an air volume is attached to the outer skin to allow outside air to enter and exit freely the ventilated cavity through the open joints. All the façade models apply vertical planes of symmetry in order to reduce the simulated volume.

Fig. 1a shows the geometry of the OJVF model for both panel arrangements: landscape (left) and portrait (right). According to the dimensions of the panels, for a 2.4-m-high façade, six panels can be installed from top to bottom in the landscape orientation, whereas only three panels in the portrait orientation. The numerical model has a geometry equivalent to two columns of panels in each case, so that both horizontal and vertical joints can be analysed in detail.

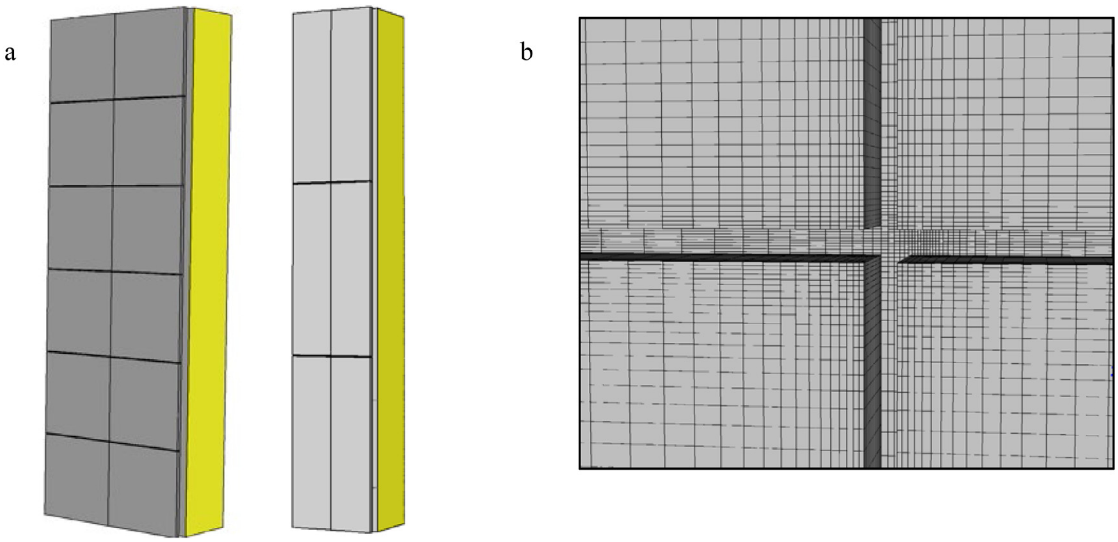

Fig. 1. (a) Geometry of the OJVF model: Landscape orientation (left) portrait orientation (right); (b) detail of the mesh in the open joints zones.

About the materials, Table 1 displays a summary of the most relevant façade features.

Table 1. Layer structure and material properties.

Wall Type	Material	Thickness (cm)	Thermal Conductivity (W/mK)	Density (kg/m^3)	Heat Capacity (J/kgK)
Outer Skin	Ceramic Panels (0.4 × 0.8 m)	2	3.5	2800	1000
Ventilated Cavity	Air	5	0.0242	Ideal gas	1006
Thermal Insulation +Inner Skin	Rockwool+ Brick +Gypsum plaster	29	0.0965	729.7	1000

The mesh discretization in these ventilated facade models is based on the main characteristics of the used in previous CFD models of the same building component [50]. The mesh is a structured grid with hexahedral cells with refined zones close to the air cavity and the open joints. In the cavity near the inner wall, the distance from the cell node to the wall was fixed to 1 mm according to the conclusions of previous sensitivity analysis [50]. This study also validated the accuracy for the calculations in the boundary layer near the walls. The optimized mesh in the landscape orientation has 2.8 million cells, whereas in the portrait one it decreases to 1.6 million, because only half of the frontal width has to be considered. Fig. 1b shows a detail of the refined mesh in the joints. An additional geometry has been developed to simulate a conventional façade with sealed cavity (base case). The dimensions of the geometry and the materials are identical to the portrait OJVF model. In this case, the mesh has 1.9 million cells. Orientations are analysed, considering both summer and winter conditions.

2.2. Numerical model and boundary conditions

The model allows the simultaneous analysis of fluid movement and heat transfer problems of OJVFs. It uses the ANSYS Fluent code to solve the Navier–Stokes equations, including the energy equation, with the finite volumes method. Following the results of previous studies [41,50], the Discrete Ordinates radiation scheme has been selected, adjusting the discretization of the solid angle in 5 divisions and 4 pixels. The turbulence effects have been included using the k-ϵ RNG turbulence equations. These models are the ones with the best adjustment between the simulated results and the experimental data obtained with Stereo-PIV methodology.

For the air, an ideal gas behaviour is assumed to calculate the density and to take into account the buoyancy effects. The properties of different layers forming the façade have been shown in Table 1. The solid materials have been considered opaque to radiation with an emissivity of 0.85 for the panels and 0.9 for the brick wall.

Regarding the boundary conditions at the inner wall, both convection and radiation to the room have been considered. Following UNE-EN-673, the convection heat transfer coefficient in this wall has been defined as 7.69 W/m2 K. The indoor comfort temperature, according to the Spanish regulations for buildings, has been fixed in 26 °C in summer conditions and in 21 °C in winter conditions. The exterior border has a constant pressure and temperature condition equal to the atmospheric and ambient values. This temperature is also used for the radiation exchange with the environment and varies according to the simulated period. About the solar radiation, both direct (perpendicular to the façade) and diffuse radiation have been considered. The values of the temperature and solar radiation for summer and winter periods are shown in Table 2 [50]. These climate data correspond to Madrid (Spain), with a Mediterranean continental climate (Köppen climate classification: Csa).

Table 2. Boundary conditions for winter and summer periods.

Period	Outdoor Temperature (ºC)	Direct Radiation (W/m^2)	Diffuse Radiation (W/m^2)	Indoor comfort Temperature (ºC)
Summer	29.5	345	214	26.0
Winter	6.0	410	197	21.0

The selection of these boundary conditions was based on a previous experimental study [50], taken as a reference, which evaluated long-term monitoring campaigns of the main climatic variables in Madrid. An average representative year for this period (2008–2018) was calculated and generated from this experimental climate file. Within this representative year, a typical summer and winter day in Madrid were calculated. These representative periods were obtained as the minimum value of a weighted sum of the registered meteorological variables, but considering the higher relevance of outdoor temperature and solar radiation variables on the performance of the façade, with weight values of 0.25 each. The data corresponding to the hours of greatest temperature difference between indoors and outdoors on these typical days, when higher ventilation rates are expected in the air chamber, were selected as boundary conditions.

With respect to the solution methodology, the energy, turbulence and radiation equations have been solved using a second order discretization scheme, and the momentum equations with a second order — pressure staggered one. The pressure–velocity coupling employs the SIMPLE algorithm. And regarding the convergence criterion, a sufficient number of iterations have been computed to ensure all the residuals were lower than 10^{-5}.

3. Results and discussion

In this research the performance of the OJVF is assessed in function of the panels' layout (landscape and portrait) in summer and winter conditions. Both arrangements are compared with a conventional sealed façade. In order to better understand the reasons behind the different behaviours, the fluid dynamic and thermal properties are analysed in detail: velocity field, air flow, panels surface temperature, heat transfer rate through the façade, etc.

The comparison between the OJVF and the conventional one is taken as a reference because the fluid-dynamic of both types of façades is clearly different, as explained in previous publications. However, the difference between the landscape and portrait orientations is more subtle, due to several reasons. On the one hand, the total opening area is the same in both orientations, but the behaviour of horizontal and vertical joints is quite different. The behaviour of the horizontal ones is more two-dimensional, affecting the entire width of the façade, while the vertical ones affect only the edges. Nevertheless, the distance between the edges in the vertical ones is much smaller, compensating for the previous effect.

In the results presented below, the fluid dynamic and thermal properties are studied in detail: velocity field, air flow, panels surface temperature, heat transfer rate through the façade, etc., in order to show the effects commented previously and analyse the global results achieved.

3.1. Velocity profiles of the air inside the cavity

The following figure show the velocity vectors in the air cavity of the landscape OJVF (Fig. 2a), the portrait OJVF (Fig. 2b) and the conventional sealed façade (Fig. 2c). In all these figures, the cross section shown is in the middle of the air cavity and perpendicular to the panels. The radiation and temperature correspond to summer conditions, which have a higher thermal load and a consequent higher cooling effect of the ventilated façades. However, the results in winter conditions are very similar and the main patterns are basically replicated.

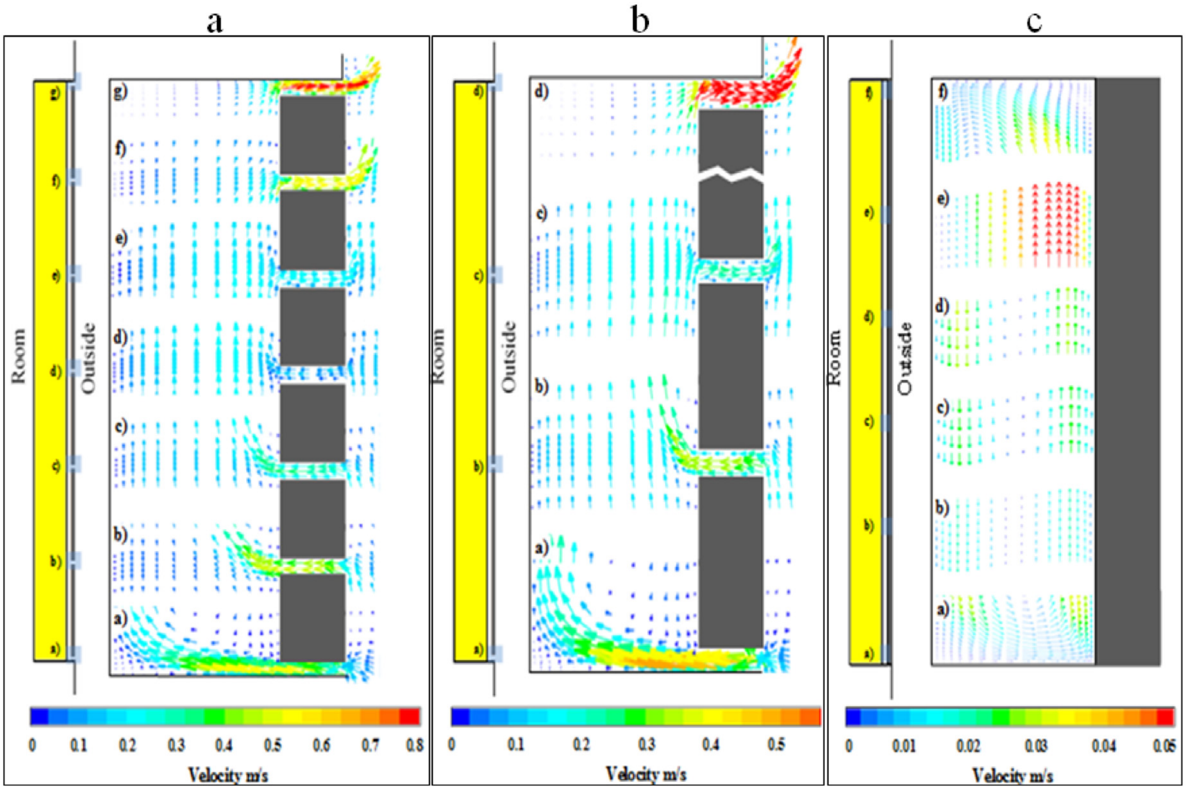

Fig. 2. Velocity vectors in summer conditions (26 °C interior, 29.5 °C exterior, 345 W/m2 direct radiation and 214 W/m2 diffuse radiation), (a) landscape OJVF; (b) portrait OJVC; (c) conventional sealed façade.

In Fig. 2a and Fig. 2b similar structures and fluid-dynamic behaviour can be observed in both arrangements (landscape and portrait). Due to the incident solar radiation on the outer layer, a natural convection phenomenon is induced generating an upward air flow. The air enters through the lower joints, creating recirculation vortexes close to the outer skin. The air ascends through the channel increasing its velocity up to the central height of the cavity. The mass flow rate has its maximum value (0.0037 kg/s) at this point. From then on, it starts to leave the cavity through the upper joints. Comparing these façades and the conventional one, the fluid-dynamic behaviour of the air is different as it shown in Fig. 2c. On one hand, the air not only ascends but forms a loop by going up against the panels and down in the area near the inner wall. On the other hand, the air not only heats up as it goes up, but also cools down as it goes down.

The highest velocities are obtained for the landscape OJVF arrangement, although the order of magnitude is quite similar to the portrait layout: about 0.25 m/s for the vertical component inside the cavity. However, the maximum velocities in the sealed cavity are one order of magnitude lower, about 0.05 m/s near the top at the panel's side.

To better understand the complex three-dimensional fluid motion inside the ventilated cavity and the flow through the joints, Fig. 3 shows the pathlines near the vertical joint at the crossing with the lower and upper horizontal ones. In the lower part of the façade (Fig. 3a), the pathlines can be seen when entering through the horizontal and the vertical joints, while in the upper part (Fig. 3b), the flow is coming out of the gap also through both of them. After going through the joints, the flow tends to separate at the exit as well as at the inlet. In the horizontal joints, the separation vortex is quite two-dimensional. However, in the vertical ones, the flow separation generates a three-dimensional twisting vortex, where the rotating motion is accompanied with a vertical displacement. Where there is flow separation, the velocity near the surface is much lower and this would affect the convection heat transfer, mainly at the interior part of the plates.

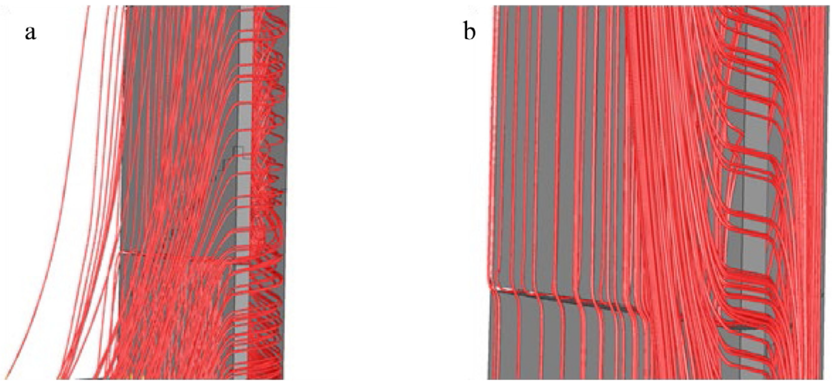

Fig. 3. Fluid pathlines through the open joints in the landscape OJVF: (a) lower part; (b) upper part.

3.2. Surface temperature of the panels

As regards the thermal behaviour, Fig. 4 shows the surface temperature of the panels for all configurations (landscape OJFV, portrait OJVF and conventional sealed façade) in both summer and winter conditions. The highest difference between winter and summer conditions is the mean temperature value, the behaviour is basically the same. In both ventilated facades, the temperature increases with height, maintaining quite similar values, but they are substantially lower than the conventional sealed façade ones. At the bottom, the flow of fresh air entering through the joints helps considerably in the cooling, making the plates cooler near the edges, both the vertical and the horizontal ones. However, at the top, the warmer airflow from the interior makes the plates a little warmer at these edges. On the upper plate, the effect of the vertical vortex can be seen. In the sealed facade, the temperature also increases with height. Due to the loop formed in the interior, the plates heat the air as it rises attached to them. There is a slight deviation from this trend at the top and bottom due to the stagnant flow in these areas.

3.3. Analysis of the heat transfer

Fig. 5 shows the heat flux in the gap in all configurations, from the panels to the air as well as from the air to the interior wall, in summer conditions. The main difference between the ventilated façades and the sealed one is the discontinuities that can be seen due to the incoming and outgoing flow through the joints. Also, in the sealed one, the heat flux from the panels to the air and from the air to the room is the same, whereas in the ventilated ones, the heat flux from the panels to the air is substantially higher than the heat flux to the interior of the room. This difference is because the ascending airflow entering and leaving the cavity through the open joints removes part of the heat reducing the heat transfer to the indoor room.

Respect to the vertical distribution, in the ventilated façades, the heat flux to the room is quite homogeneous although with a small increase from bottom to top. The heat flux from the panels to the air is much higher at the

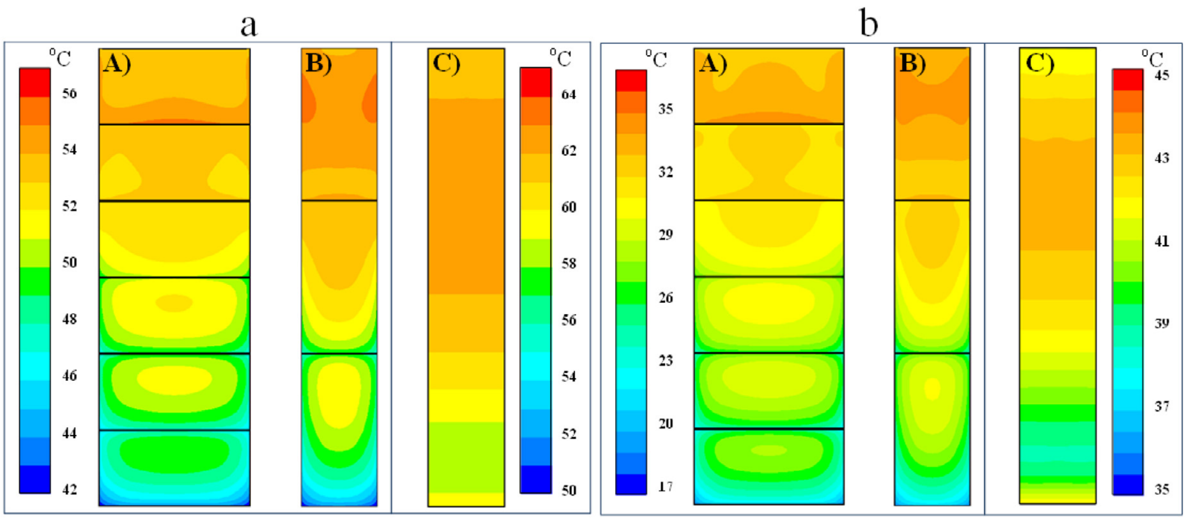

Fig. 4. Panels' temperature in (a) summer and (b) winter conditions: (A) landscape OJVF; (B) portrait OJVF and (C) conventional sealed façade.

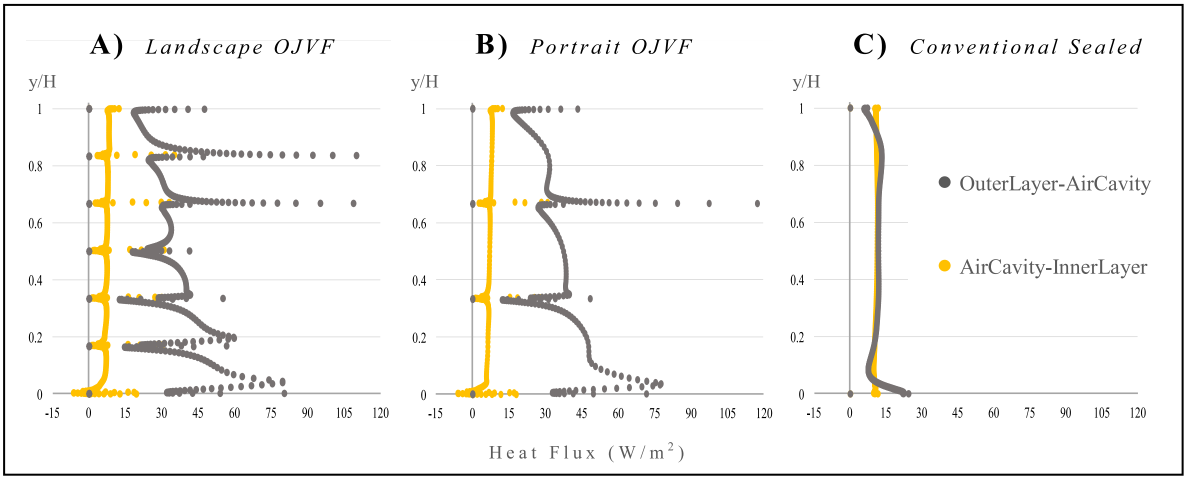

Fig. 5. Heat flux in the air cavity in all configurations and summer conditions: (a) landscape OJVF (b) portrait OJVF and (c) conventional sealed façade. y/H are position coordinates normalized by cavity height (H=2.4 m).

bottom; although the panels' temperature is lower, there is a higher temperature difference between the panels and the air. In the sealed one, the heat flux is also more relatively homogeneous from the air to the interior of the room, while greater variations can be seen from the panels to the air, especially in the lower and upper part due to the stagnation in the rotation of the loop and the temperature difference with height.

Regarding the difference between summer and winter conditions and also, the horizontal distribution, these results can be seen in Fig. 6. They present the heat flux to the interior of the room in all configurations in both conditions. In summer, the heat flux is higher than in winter. Also, the sealed façade has much higher heat flux than the ventilated ones in both conditions. The heat flux always increases from bottom to top, but not much. The highest differences can be found in the ventilated façades in summer conditions. About the horizontal distribution, there is little variation in the heat flux with the width. A small difference can be seen in the ventilated façades, but much smaller than the vertical changes.

Table 3 shows the total heat flux to the building, calculated in both summer and winter conditions. As it can be seen, the ventilated façades are very similar and they allow much less heat transfer than the conventional one, about

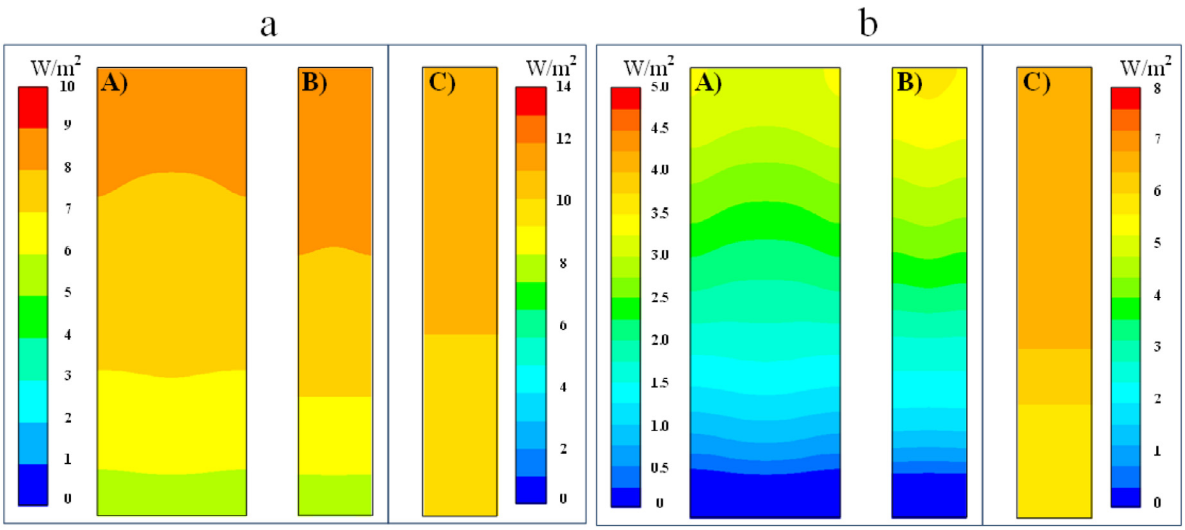

Fig. 6. Heat flux to the room in (a) summer and (b) winter conditions: (A) landscape OJVF; (B) portrait OJVF, (C) conventional sealed façade.

Table 3. Total heat flux to the building.

Configuration	Summer Heat Flux (W/m^2)	Winter Heat Flux (W/m^2)
Landscape OJVF	7.30	1.81
Portrait OJVF	7.53	2.01
Conventional façade	10.89	6.38

30% less in summer and 70% less in winter. The differences between ventilated façades are quite small. However, the landscape arrangement has a slightly better performance, its heat transfer is 3% lower in summer and 10% lower in winter.

4. Conclusions

The façade of a building is a critical component regarding its thermal performance. For this reason, it is important to optimize its design minimizing the heat exchanges between the building and the environment. To this end, two real OJVFs with landscape and portrait arrangements and a conventional sealed façade have been comparatively analysed.

A CFD model, previously validated with experimental data, has been used to study the orientation of the panels in OJVFs. The DO radiation model and k-ε RNG turbulence model have been utilized together with the solar radiation (direct and diffuse) introduced explicitly at the boundary condition in the domain. Three-dimensional numerical simulations have been performed in summer and winter conditions determining the main features of the thermal and fluid behaviour of these façades.

The analysis of the results shows similar temperature trends along the whole height in OJVFs, regardless of the different panels' arrangement (landscape or portrait); with an exterior surface temperature about 10oC lower than the conventional one. The behaviour of the air inside the cavity in OJVFs is a complex three dimensional ventilation airflow induced by natural convection, in contrast to the two-dimensional closed vortex inside the gap of the conventional façade. In addition, the magnitude of the velocity is significantly smaller.

With respect to the heat transfer into the room, both ventilated arrangements are much more efficient than the sealed one, allowing about 30% less heat transfer in summer. Comparing the arrangements of the panels, the differences are not very big, but the landscape one maximizes the heat exchange with the airflow, minimizing the heat transferred to the building in the summer period. In these conditions, the landscape orientation is 3% more efficient than the portrait one.

The main result in terms of practical application can be that the most important criterion in the choice of the panel orientation, as the differences between them are small, is aesthetics, not energy performance. But, regarding the energy criterion, the best solution would be envelopes with a higher percentage of openings in landscape orientation.

Declaration of competing interest

The authors declare the following financial interests/personal relationships which may be considered as potential competing interests: Maria Nuria Sanchez y Maria Jose Jimenez reports financial support was provided by Spanish National Research Agency.

Data availability

Data will be made available on request.

Acknowledgement

This research was funded by the Spanish National Research Agency (Agencia Estatal de Investigación) through the In-Situ-BEPAMAS project (PID2019-105046RB-I00/AEI/10.13039/501100011033).

References

[1] Juaristi M, Favoino F, Gómez-Acebo T, Monge-Barrio A. Adaptive opaque façades and their potential to reduce thermal energy use in residential buildings: A simulation-based evaluation. J Build Phys 2022;45(5):675–720.
[2] Assoa YB, Thony P, Messaoudi P, Schmitt E, Bizzini O, Gelibert S, et al. Study of a building integrated bifacial photovoltaic facade. Sol Energy 2021;227:497–515.
[3] Yitmen I, Al-Musaed A, Yücelgazi F. ANP model for evaluating the performance of adaptive façade systems in complex commercial buildings engineering. Constr Archit Manag 2021;29(1):431–55.
[4] Martín-Gómez C, Zuazua-Ros A, Del Valle de Lersundi K, Sánchez Saiz-Ezquerra B, Ibáñez Puy M. Integration development of a ventilated active thermoelectric envelope (VATE): Constructive optimization and thermal performance. Energy Build 2021;231:110593.
[5] Lee H, Ozaki A, Choi Y, Iqbal M. Performance improvement plan of air circulation-type solar heat-storage system using ventilated cavity of roof. Energies 2021;14(6):1606.
[6] Balter J, Barea G, Ganem C. Improvements in the energy performance of buildings in summer through the integration of ventilated envelopes on north-facing facades and roofs. Habitat Susten 2020;10(2):94–105.
[7] Ahmad RM, El-Sayed Z, Taha D, Shokry H, Mahmoud H. An approach to select an energy-efficient shading device for the south-oriented façades in heritage buildings in Alexandria. Egypt Energy Rep 2021;7:133–7.
[8] Carlini M, Castellucci S, Ceccarelli I, Rotondo M, Mennuni A. Study of a thermal dispersion in buildings and advantages of ceramic coatings for the reduction of energy expenditure. Energy Rep 2020;6:116–28.
[9] Yang Z, Tu Y, Ma H, Yang X, Liang C. Numerical simulation of a novel double-duct ventilation system in poultry buildings under the winter condition. Build Environ 2022;207:108557.
[10] Soutullo S, Sánchez MN, Enríquez R, Olmedo R, Jiménez MJ. Bioclimatic vs conventional building: experimental quantification of the thermal improvements. Energy Proc 2017;122:823–8.
[11] Utkucu D, Sözer H. An evaluation process for natural ventilation using a scenario-based multi-criteria and multi-interaction analysis. Energy Rep 2020;6:644–61.
[12] Albatayneh A. Optimisation of building envelope parameters in a semi-arid and warm mediterranean climate zone. Energy Rep 2021;7:2081–93.
[13] Rahiminejad M, Khovalyg D. Review on ventilation rates in the ventilated air-spaces behind common wall assemblies with external cladding. Build Environ 2021;190:107538.
[14] Domínguez-Torres C-A, León-Rodríguez ÁL, Suárez R, Domínguez-Delgado A. Empirical and numerical analysis of an opaque ventilated facade with windows openings under mediterranean climate conditions. Mathematics 2022;10(163).
[15] Saroglou T, Theodosiou T, Givoni B, Meir IA. Studies on the optimum double-skin curtain wall design for high-rise buildings in the Mediterranean climate. Energy Build 2020;208:109641.
[16] Preet S, Mathur J, Mathur S. Influence of geometric design parameters of double skin façade on its thermal and fluid dynamics behavior: A comprehensive review. Sol Energy 2022;236:249–79.
[17] Pastori S, Mereu R, Mazzucchelli ES, Passoni S, Dotelli G. Energy performance evaluation of a ventilated façade system through CFD modeling and comparison with international standards. Energies 2021;14(1):193.
[18] Jankovic A, Siddiqui MS, Goia F. Laboratory testbed and methods for flexible characterization of thermal and fluid dynamic behaviour of double skin facades. Build Environ 2022;210:108700.
[19] Sotelo-Salas C, Pozo CE-D, Esparza-López CJ. Thermal assessment of spray evaporative cooling in opaque double skin facade for cooling load reduction in hot arid climate. J Build Eng 2021;38:102156.
[20] Girma GM, Tariku F. Experimental investigation of cavity air gap depth for enhanced thermal performance of ventilated rain-screen walls. Build Environ 2021;194:107710.

[21] Zhang W, Gong T, Ma S, Zhou J, Zhao Y. Study on the influence of mounting dimensions of pv array on module temperature in open-joint photovoltaic ventilated double-skin façades. Sustainability 2021;13(9):5027.
[22] Wang Y, Chen Y, Li C. Airflow modeling based on zonal method for natural ventilated double skin façade with venetian blinds. Energy Build 2019;191:211–23.
[23] Pizzatto SMDS, Pizzatto FO, Angioletto E, Arcaro S, Junca E, Klegues Montedo OR. Thermal evaluation of the use of porous ceramic plates on ventilated façades—part II: Thermal behavior. Int J Appl Ceram Technol 2021;18(5):1734–42.
[24] Nizovtsev MI, Letushko VN, Borodulin VYu, Sterlyagov AN. Experimental studies of the thermo and humidity state of a new building facade insulation system based on panels with ventilated channels. Energy Build 2020;206:109607.
[25] Pujadas-Gispert E, Alsailani M, van Dijk KCA, Rozema ADK, ten Hoope JP, Korevaar CC, et al. Design construction, and thermal performance evaluation of an innovative bio-based ventilated façade. Front Archit Res 2020;9(3):681–96.
[26] Blanco JM, Buruaga A, Cuadrado J, Zapico A. Assessment of the influence of facade location and orientation in indoor environment of double-skin building envelopes with perforated metal sheets. Build Environ 2019;163:106325.
[27] Ling H, Wang L, Chen C, Chen H. Numerical investigations of optimal phase change material incorporated into ventilated walls. Energy 2019;172:1187–97.
[28] Benzarti S, Chaabane M, Mhiri H, Bournot P. Performance improvement of a naturally ventilated building integrated photovoltaic system using twisted baffle inserts. J Build Eng 2022;53:104553.
[29] Agathokleous RA, Kalogirou SA. Status barriers and perspectives of building integrated photovoltaic systems. Energy 2020;191:116471.
[30] Cuce E, Cuce PM. Optimised performance of a thermally resistive PV glazing technology: An experimental validation. Energy Rep 2019;5:1185–95.
[31] Theokli C, Elia C, Markou M, Vassiliades C. Energy renovation of an existing building in nicosia cyprus and investigation of the passive contribution of a BIPV/T double façade system: A case-study. Energy Rep 2021;7:8522–33.
[32] Gagliano A, Nocera F, Aneli S. Thermodynamic analysis of ventilated facades under different windconditions in summer period. Energy Build 2016;122:131–9.
[33] Colinart T, Bendouma M, Glouannec P. Building renovation with prefabricated ventilated façade element: A case study. Energy Build 2019;186:221–9.
[34] Juaristi M, Gómez-Acebo T, Monge-Barrio A. Qualitative analysis of promising materials and technologies for the design and evaluation of Climate Adaptive Opaque Façades. Build Environ 2018;144:482–501.
[35] Stazi F, Ulpiani G, Pergolini M, Di Perna C, D'Orazio M. The role of wall layers properties on the thermal performance of ventilated facades: Experimental investigation on narrow-cavity design. Energy Build 2020;209:109622.
[36] Fantucci S, Marinosci C, Serra V, Carbonaro C. Thermal performance assessment of an opaque ventilated façade in the summer period: calibration of a simulation model through in-field measurements. Energy Procedia 2017;111:619–28.
[37] Stazi F, Ulpiani G, Pergolini M, Magni D, Di Perna C. Experimental comparison between three types of opaque ventilated facades. Open Constr Build Technol J 2018;12:296–308.
[38] Lin Z, Song Y, Chu Y. An experimental study of the summer and winter thermal performance of an opaque ventilated facade in cold zone of China. Build Environ 2022;218:109108.
[39] Fantucci S, Serra V, Carbonaro C. An experimental sensitivity analysis on the summer thermal performance of an opaque ventilated façade. Energy Build 2020;225:110354.
[40] Gagliano A, Aneli S. Analysis of the energy performance of an opaque ventilated facade under winter and summer weather conditions. Sol Energy 2020;205:531–44.
[41] Sánchez MN, Giancola E, Suárez MJ, Blanco E, Heras MR. Experimental evaluation of the airflow behaviour in horizontal and vertical open joint ventilated facades using stereo-PIV. Renew Energy 2017;109:613–23.
[42] Sanjuan C, Sánchez MN, Enriquez R, Heras MR. Experimental PIV techniques applied to the analysis of natural convection in open joint ventilated facades. Energy Procedia 2012;30:1216–25.
[43] Sánchez MN, Sanjuan C, Suárez MJ, Heras MR. Experimental assessment of the performance of open joint ventilated façades with buoyancy-driven airflow. Sol Energy 2013;91:131–44.
[44] Garafolo NG, Wittmer J, Pathak S. Curvature correction applied to droplets subjected to natural convection for particle image velocimetry. Colloids Surf Physicochem Eng Asp 2020;597:124442.
[45] Giancola E, Sánchez MN, Friedrich M, Larsen OKalyanova, Nocente A, Avesani S, et al. Possibilities and challenges of different experimental techniques for airflow characterisation in the air cavities of façades. J Facade Des Eng 2018;6(3):34–48.
[46] Sanjuan C, Sánchez MN, Heras MR, Blanco E. Experimental analysis of natural convection in open joint ventilated facades with 2D PIV. Build Environ 2011;46:2314–25.
[47] Sánchez MN, Giancola E, Blanco E, Soutullo S, Suárez MJ. Experimental validation of a numerical model of a ventilated façade with horizontal and vertical open joints. Energies 2020a;13(1):146.
[48] Suárez MJ, Sanjuan C, Gutiérrez AJ, Pistono J, Blanco E. Energy evaluation of a horizontal open joint ventilated façade. Appl Therm Eng 2012;37:302–13.
[49] Giancola E, Sanjuan C, Blanco E, Heras MR. Experimental assessment and modelling of the performance of an open joint ventilated façade during actual operating conditions in mediterranean climate. Energy Build 2012;54:363–75.
[50] Sánchez MN, Soutullo S, Olmedo R, Bravo D, Castaño S, Jiménez MJ. An experimental methodology to assess the climate impact on the energy performance of buildings: A ten-year evaluation in temperate and cold desert areas. Appl Energy 2020b;264:114730.